PDE3A mutations cause autosomal dominant hypertension with brachydactyly

Maass, P.G., Aydin, A., Luft, F.C., Schaechterle, C., Weise, A., Stricker, S., Lindschau, C., Vaegler, M., Qadri, F., Toka, H.R., Schulz, H., Krawitz, P.M., Parkhomchuk, D., Hecht, J., Hollfinger, I., Wefeld-Neuenfeld, Y., Bartels-Klein, E., Muehl, A., Kann, M., Schuster, H., Chitayat, D., Bialer, M.G., Wienker, T.F., Ott, J., Rittscher, K., Liehr, T., Jordan, J., Plessis, G., Tank, J., Mai, K., Naraghi, R., Hodge, R., Hopp, M., Hattenbach, L.O., Busjahn, A., Rauch, A., Vandeput, F., Gong, M., Rueschendorf, F., Huebner, N., Haller, H., Mundlos, S., Bilginturan, N., Movsesian, M.A., Klussmann, E., Toka, O., Baehring, S.

This is the final version of the accepted manuscript. The original article has been published in final edited form in:

Nature Genetics
2015 JUN ; 47(6): 647-653
doi: 10.1038/ng.3302
Nature Publishing Group

PDE3A mutations in autosomal-dominant hypertension with brachydactyly

Running head: genetic hypertension

Philipp G. Maass[1, 2, 30], Atakan Aydin[1, 2, 30], Friedrich C. Luft[1, 2, 3, 30*], Carolin Schächterle[2, 30], Anja Weise[4], Sigmar Stricker[5,6], Carsten Lindschau[7, 8], Martin Vaegler[9], Fatimunnisa Qadri[1, 2], Hakan R. Toka[10], Herbert Schulz[2, 11], Peter M. Krawitz[5, 12, 13], Jochen Hecht[5, 13], Irene Hollfinger[2], Yvette Wefeld-Neuenfeld[2], Eireen Bartels-Klein[2], Astrid Mühl[2], Martin Kann[14], Herbert Schuster[15], David Chitayat[16, 17], Martin G. Bialer[18], Thomas F. Wienker[5], Jürg Ott[19], Katharina Rittscher[4], Thomas Liehr[4], Jens Jordan[20], Ghislaine Plessis[21], Jens Tank[20], Knut Mai[1], Ramin Naraghi[22], Russell Hodge[2], Maxwell Hopp[23], Lars O. Hattenbach[24], Andreas Busjahn[1, 25], Anita Rauch[26], Fabrice Vandeput[27], Maolian Gong[2], Franz Rüschendorf[2], Norbert Hübner[2], Hermann Haller[7], Stefan Mundlos[5, 12, 13], Nihat Bilginturan[28], Matthew A. Movsesian[27], Enno Klussmann[2], Okan Toka[29], and Sylvia Bähring[1, 2, 30]

[1] Experimental and Clinical Research Center (ECRC), a joint cooperation between the Charité Medical Faculty and the Max Delbrück Center for Molecular Medicine (MDC), Lindenbergerweg 80, 13125 Berlin, Germany

[2] Max Delbrück Center for Molecular Medicine (MDC), Robert-Rössle-Strasse 10, 13125 Berlin, Germany

[3] Department of Medicine, Division of Clinical Pharmacology, Vanderbilt University School of Medicine, Nashville, TN, USA

[4] Jena University Hospital, Friedrich Schiller University, Institute of Human Genetics, Kollegiengasse 10, 07743, Jena, Germany

[5] Max Planck Institute for Molecular Genetics, Ihnestrasse 73, 14195 Berlin, Germany

[6] Institute for Chemistry and Biochemistry, Freie Unversität Berlin, Thielallee 63, 14195 Berlin, Germany

[7] Department of Nephrology, Hannover University Medical School, Hannover, Germany

[8] Staatliche Technikerschule Berlin, Bochumer Strasse 8, 10555 Berlin

[9] University Department of Urology, Laboratory of Tissue Engineering, Eberhard Karls University Tübingen, Paul-Ehrlich-Strasse 15, 72076 Tübingen, Germany

[10] Eastern Virginia Medical School, Division of Nephrology and Hypertension, 855 W Brambleton Ave, Norfolk, VA 23510, USA; Brigham and Women's Hospital, Division of Nephrology, 75 Francis Street, MRB4, Boston, MA 02215, USA

[11] University of Cologne, Cologne Center for Genomics (CCG), Weyertal 115 B, Cologne, Germany

[12] Institute for Medical Genetics and Human Genetics, Charité, Universitätsmedizin Berlin, 13353 Berlin, Germany

[13] Berlin Brandenburg Center for Regenerative Therapies (BCRT), Charité, Universitätsmedizin Berlin, 13353 Berlin, Germany

[14] Department of Nephrology, School of Medicine, University of Cologne, Germany

[15] INFOGEN, Xantener Strasse 10, 10707 Berlin

[16] The Hospital for Sick Children, Division of Clinical and Metabolic Genetics, University of Toronto, Toronto, Ontario, Canada

[17] The Prenatal Diagnosis and Medical Genetics Program, Department of Obstetrics and Gynecology, Mount Sinai Hospital, University of Toronto, Toronto, Ontario, Canada

[18] Division of Medical Genetics and Department of Pediatrics, North Shore/LIJ Health System, Manhasset, NY, USA

[19] Statistical Genetics, Rockefeller University New York, NY, USA, and Institute of Psychology, Chinese Academy of Sciences, Beijing, China

[20] Institute of Clinical Pharmacology, Hannover Medical School, Carl-Neuberg-Str. 1, 30625 Hannover, Germany

[21] Centre Hospitalier Universitaire de Caen, Cytogénétique postnatale et génétique Clinique, Avenue George Clemenceau, Caen, France

[22] Department of Neurosurgery, Bundeswehrkrankenhaus Ulm, 89081 Ulm, Germany

[23] Griffith Base Hospital, Department of Pediatrics, Griffith, NSW, Australia

[24] Department of Ophthalmology, Hospital Ludwigshafen, Ludwigshafen, Germany

[25] HealthTwist GmbH, Lindenberger Weg 80, 13125 Berlin, Germany

[26] Institute for Medical Genetics, University of Zurich, Switzerland

[27] Cardiology Section, VA Salt Lake City Health Care System; Departments of Internal Medicine and Pharmacology and Toxicology, University of Utah, Salt Lake City, UT, USA

[28] Department of Pediatric Endocrinology, Hacettepe University, Turkey

[29] Childrens Hospital, Department of Pediatric Cardiology, Friedrich-Alexander University Erlangen, Loschge Strasse 15, 91054 Erlangen, Germany

[30] The authors contributed equally to this work.

* Corresponding author:

Friedrich C. Luft, MD

Lindenberger Weg 80

13125 Berlin, Germany

Phone: +49 30 450 540 001

Fax: +49 30 450 540 900

Mail: luft@charite.de

Word count without introductory paragraph, methods summary, acknowledgements, author contributions and figure legends: 1749

Cardiovascular disease is the commonest cause of death worldwide and hypertension is the major risk factor;[1] Mendelian hypertension elucidates mechanisms of blood pressure regulation. We identified six missense mutations in phosphodiesterase 3A (*PDE3A*) in six unrelated families with Mendelian hypertension and brachydactyly Type E (HTNB)[2] by whole-genome sequencing. The syndrome features brachydactyly Type E (BDE), short stature, severe salt-independent but age-dependent hypertension, increased fibroblast growth rate, neurovascular contact at the rostral ventrolateral medulla, altered baroreflex blood pressure regulation, and death from stroke before age 50 when untreated.[3,4] The *PDE3A* mutations resulted in gain-of-function, with increased cAMP-hydrolytic affinity, and enhanced cell proliferation. The mutations increased protein kinase A (PKA)-mediated PDE3A phosphorylation. Mesenchymal stem cell-derived vascular smooth muscle cells (VSMC) and chondrocytes provided insights into the molecular pathogenesis of HTNB; PDE3A phosphorylation was enhanced, vasodilator-

stimulated phosphoprotein (VASP) was diminished, while parathyroid hormone-related peptide (PTHrP) was dysregulated. We suggest that the identified *PDE3A* mutations cause the syndrome. VSMC-expressed PDE3A deserves scrutiny as a therapeutic target.

All Mendelian hypertension syndromes described to date involve increased sodium reabsorption in the distal nephron.[5] The sole exception is autosomal-dominant hypertension with BDE (HTNB, OMIM #112410), first reported in a Turkish kindred.[2,6] HTNB was linked to chromosome 12p in six unrelated families.[2,7,8] The locus accounts for a ~50 mm Hg mean blood pressure difference at age 50 years.[2] The penetrance is 100% (Fig. 1a). Previously, we reported a rearrangement on chromosome 12p common to all families.[8,9] A linkage study in Chinese hypertensive families without BDE coincided with the HTNB locus, supporting relevance to essential hypertension.[10]

Whole-genome sequencing of Turkish family members revealed a heterozygous missense mutation in *PDE3A* (Gene ID: 5139), a gene encoding a cGMP/cAMP phosphodiesterase with a prominent role in the heart, VSMC, oocytes and platelets.[11] Re-sequencing of all 48 affected persons in six unrelated families identified six independently clustered heterozygous missense mutations in exon 4 (Fig. 1a, b, 2a, Supplementary Table 1). The mutational amino acids 445, 447, and 449 belong to a highly conserved *PDE3A* domain (Supplementary Fig. 1).

We detected none of the previously described chromosomal breakpoints on chromosome 12p12.2-12.1, perhaps due to high repetitive content in the breakpoint regions (Fig. 2a, Supplementary Table 2).[8,9] Intra-familial variability was noted with an affected individual (VI/9, 145/77 mm Hg) showing only mild BDE with height (159 cm) in the 30th percentile compared to one of his severely affected cousins (142 cm, 1st percentile, VI/1; Fig.

2b).[7] Magnetic resonance imaging revealed a posterior-inferior cerebellar artery (PICA) loop (Supplementary Fig. 2a-c).[4] A haplotype analysis identified a novel recombination that reduced the linkage interval and eliminated an inversion common to all affected individuals in the six families (Fig. 2c).[9] In contrast, the affected mother's haplotype showed co-segregation with the more severe brachydactyly phenotype.

PDEs are involved during early stages of osteogenesis.[12] *PDE4D* mutations have been associated with severe brachydactyly in acrodysostosis.[13,14] In mice, *Pde3a* was expressed in the developing limbs, consistent with a role during chondrogenesis (Fig. 2d, Supplementary Fig. 3a, b). Chondrogenic downregulation of *PTHLH* encoding PTHrP was associated with BDE.[15] We also observed *PTHLH* downregulation in chondrogenically induced fibroblasts from affected persons (Fig. 2e, Supplementary Fig. 3c).

We addressed the functional consequences of the identified *PDE3A* mutations in HeLa cells expressing the six mutations. Forskolin or L-arginine stimulated the adenylate or guanylate cyclases to enhance cellular cAMP or cGMP levels, respectively.[16,17] We detected significantly reduced cAMP levels, consistent with gain-of-function mutations with no change in cGMP levels for the PDE3A mutations (Supplementary Fig. 4a, b). Three PDE3A isoforms, PDE3A1 (microsomal), PDE3A2 and PDE3A3 (microsomal and cytosolic), have been identified in human myocardium.[18,19] PDE3A3 does not contain the sequence harboring the detected mutations. The predominant isoform in VSMC is PDE3A2.[18,20] To directly elucidate the mutations' effects, we compared the Michaelis-Menten kinetics of cAMP-hydrolytic activity for recombinant T445N FLAG-tagged PDE3A1 and PDE3A1-WT and the tagged A2 isoforms purified from transfected cells (Fig. 3a, b, Supplementary Fig. 4d-k). The T445N mutation increased the affinity of both enzyme's isoforms for cAMP (decreased K_M) without affecting V_{max}; this increase in affinity relative to the wildtype enzyme was enhanced

for both isoforms when cAMP-mediated signaling in transfected cells was stimulated by exposure to forskolin. IC_{50} measurements for milrinone, a PDE3 inhibitor, used to augment cardiac contractility and decrease vascular resistance in patients with heart failure,[21,22] showed that higher concentrations of the inhibitor were necessary to inhibit both isoforms of the recombinant T445N PDE3A mutants (Fig. 3c, d), while the IC_{50} values for cGMP inhibition of cAMP-hydrolytic activity were nearly equivalent for wildtype and mutational enzyme (Supplementary Fig. 5).

We also used a luciferase vector under the control of a cAMP-responsive element to determine the effects of all six *PDE3A* mutations on cAMP-mediated signaling in cells.[23] Consistent with the observed gain-of-function effect and due to the resulting increased cAMP-hydrolytic activity, expression of all six *PDE3A* mutations decreased luciferase expression compared to wildtype (Supplementary Fig. 6a-g).

We extracted mesenchymal stem cells (MSC) from two affected individuals with the mutation T445N (VI/9, VI/17). MSC were FACS-characterized and differentiated into adipocytes, osteocytes, and chondrocytes demonstrating their multilineage potential (Supplementary Fig. 7a, b).[24] MSC-derived VSMC expressed smooth muscle actin alpha (SMAα), calponin, and transgelin at high levels (SM22α; Supplementary Fig. 7c). Because deleted murine *Pde3a* suppressed VSMC proliferation, indicating its importance during arteriogenesis and arterial remodeling[25], we focused on the vascular relevance of the *PDE3A* mutations. In our earlier studies, we had observed an enhanced cell growth rate of affected person's fibroblasts and hyperplastic blood-vessel walls, concerning the thickened VSMC layer.[9,26] We hypothesized that the *PDE3A* mutations were responsible for enhanced mitosis and arterial remodeling. In HeLa proliferation assays with *PDE3A* full-length transfected constructs, as well as in T445N patient-derived VSMC, we determined higher mitotic rates.

Transfected wildtype PDE3A increased also cell growth compared to endogenous PDE3A (Fig. 3e, f, Supplementary Fig. 8).

Near the *PDE3A* mutations, the residues $Ser^{428+438}$ can be phosphorylated by protein-kinase C (PKC) or PKA, causing increased cAMP hydrolysis (Fig. 2a).[18,27,28] Thus, we investigated phosphorylated PDE3A without and after exposure to PMA (to activate PKC) or forskolin (to yield activated PKA).[29,30] The phosphorylation of mutational PDE3A1 and PDE3A2 at Ser^{428} and Ser^{438} was increased in PMA- and forskolin-treated HeLa cells, compared to endogenous and transfected wildtype PDE3A (Fig. Fig. 4a-e, Supplementary Fig. 9).[19] In non-stimulated MSC and VSMC of the affected T445N patients, higher PDE3A Ser^{428} and Ser^{438} phosphorylation was detected (Fig. 4f, g). Inhibiting PKA or PKC showed that both kinases phosphorylated PDE3A Ser^{438} (Supplementary Fig. 10). We investigated whether or not the altered PDE3A phosphorylation could be attributed to a favored mRNA expression from the affected allele. We used pyrosequencing to dissect the allele usage and detected no differences (Supplementary Fig. 11).

Reduced phosphorylation of VASP at Ser^{157}, mediated by PKA, has been linked to enhanced VSMC proliferation after angioplasty.[31] Elevated full-length PTHrP enhanced neointimal proliferation, while the PTHrP peptide [1-36] inhibited VSMC proliferation.[31,32] We observed reduced VASP Ser^{157} phosphorylation and elevated PTHrP in PMA-stimulated HeLa cells expressing the mutational enzymes. VASP Ser^{157} phosphorylation was not greatly altered in forskolin-treated HeLa, most likely due to increased forskolin-induced cAMP levels that are sufficient for PKA activation despite hyperactive PDE3A (Fig. 4h). Moreover, increased expression of PTHrP full-length protein and decreased PTHrP peptide [1-36] were detected in affected persons' cells (Supplementary Fig. 12).

In a peptide-SPOT assay, we synthesized 30-mer peptides representing Ile^{421}-Leu^{450} of PDE3A wildtype and the six mutations including alanine and asparagine replacements for $Ser^{428+438}$ (Fig. 2a, 5a, Supplementary Fig. 13).[33] The spotting of Ser^{438} or pre-phosphorylated serines at position 428 or 438, followed by PKA *in vitro* phosphorylation of Ser^{438}, revealed significantly enhanced phosphorylation at the PDE3A Ser^{438} residue of the six mutants, confirming the previous results (Fig. 5a, b, Supplementary Fig. 14a-c). To further elucidate the increased phosphorylation signal at the pre-phosphorylated Ser^{438} residue (peptide lanes' 7 and 9), we examined whether PKA additionally phosphorylated further residues. Interestingly, the PKA signals increased even though Ser^{428} and Ser^{438} were substituted with alanine. This result could be due to increased phosphorylated Ser^{439} and Thr^{440}, being close to Ser^{438} (Supplementary Fig. 14d-f).

Finally, we substituted Ser^{428}, Ser^{438}, Ser^{439} and Thr^{440} with alanines and repeated the Michaelis-Menten kinetics of FLAG-tagged PDE3A1 and PDE3A2 WT versus the T445N mutant. The alanine substitutions led to reduced cAMP affinity. We measured enhanced K_M values for the substituted isoforms, supporting the notion that the mutation-dependent enhanced phosphorylations at these sites were responsible for the increased cAMP affinity and hydrolysis (Fig. 5c, Supplementary Fig. 15).

We observed that PDE3A mutated at residues Ser^{428} and Ser^{438} was more extensively phosphorylated than wildtype PDE3A, and that PTHrP isoforms were dysregulated. Our results suggest that the increased PKA-phosphorylation at Ser^{438} and PKC-phosphorylation of Ser^{428}, reported to increase PDE3A2 activity,[27] may have contributed to the increase in the cAMP-hydrolytic activity of the mutational enzymes, leading to reduced cAMP levels and enhanced cell proliferation. This result would be consistent with the increased affinity of the T445N-mutant for cAMP we observed following exposure of transfected cells to forskolin

(Fig. 3a, b). Further important studies will aim to characterize the possible allosteric effects of these mutations on other phosphorylation sites that may modulate activity and on protein-protein interactions involved in PDE3A function – for example, the interaction of PDE3A with phospholamban, SERCA2 and AKAP18 described in mouse heart.[34,35]

Augmented full-length PTHrP, decreased PTHrP peptide [1-36] and reduced VASP phosphorylation could additionally promote VSMC proliferation, leading to vessel wall hyperplasia. In our functional assays, we determined the gain-of-function effect for the PDE3A mutants. The observed IC_{50} values showed that a higher milrinone concentration was necessary to abrogate the increased PDE3A1 and PDE3A2 T445N cAMP hydrolysis. In luciferase assays, the inhibitors given alone were not sufficient to block the gain-of-function effect. These data are compatible with our previous results indicating that milrinone-induced forearm vasodilation in affected persons and controls were not significantly different.[8]

Our data strongly suggest that *PDE3A* mutations in HTNB are responsible for the hypertension by contributing to a general increase in peripheral vascular resistance (Fig. 5d).[2,26] The fact that PDE3 inhibition lowers blood pressure in hypertensive heart failure patients and in patients with pulmonary hypertension is consistent with this hypothesis.[36] cAMP inhibits myosin light-chain kinase (MLCK) through the phosphorylation of the latter by PKA, thereby causing VSMC relaxation. Dephosphorylation of myosin light chains by MLC phosphatase also produces relaxation.[37] Enhanced PDE3A activity could, by lowering intracellular [cAMP] in VSMC, promote increased peripheral vascular constriction. Furthermore, increased VSMC proliferation could induce remodeling favoring hypertension, perhaps by vascular structural changes or neurovascular contact. Our studies of PDE3A mutants with increased activity showing enhanced mitosis are consistent with the observed decrease in VSMC proliferation when deleting PDE3A in an earlier study.[25]

The milder BDE of subject VI/9 suggests that regulatory DNA elements or non-coding RNA of the excluded inversion region epigenetically trigger the BDE and short stature pathogenesis. We found that *Pde3a,* involved in murine chondrogenesis, could contribute to *PTHLH* downregulation that was associated with BDE.[15,38] In chondrocytes, PTHrP is regulated by cAMP and transduces signals through the PTH/PTHrP receptor, activating adenylate cyclase for cAMP production.[39,40] We suggest that increased cAMP hydrolysis could cause PTHrP downregulation through a regulatory feedback loop (Fig. 5d).

In conclusion, we have identified independently clustered *PDE3A* mutations in HTNB individuals, exhibiting a gain-of-function effect on cAMP hydrolysis. We found evidence for mechanisms mediating VSMC hyperplasia and increased peripheral vascular resistance. The functional consequences of the *PDE3A* mutations in animal models will result in further insight into the normal and pathogenic vascular and skeletal development.

Methods summary

We studied six unrelated families. After approval by the ethics committee (Charité Medical Faculty, Berlin) and written, informed consent, we obtained skin fibroblasts from 6 affected persons (3 ♂, 3 ♀) and 8 controls (5 ♂, 3 ♀) from the Turkish kindred; mean age was 37.7±0.4 years. We extracted mesenchymal stromal cells (MSC) from two affected Turkish males (VI/9, 17 years and VI/17, 12 years) and two non-affected and non-related (♂: 15, ♀: 59 years) controls. Additional methods are described in the supplements.

Acknowledgements

We thank all family members for their cooperation. We thank May-Britt Köhler and Mohammad Toliat for technical assistance. The Deutsche Forschungsgemeinschaft (DFG)

(BA1773/4-1, BA1773/4-2, MA5028/1-2, MA5028/1-3), grants-in-aid from the German Hypertension Society (Deutsche Hochdruckliga e.V. DHL®), and from the German Heart Research Foundation (F/24/13) supported PGM, FCL, OT, and SB. The DFG (KL1415/4-2), the Else Kröner-Fresenius-Stiftung (2013_A145), and the German-Israeli Foundation (I-1210-286.13/2012) supported EK. The US Department of Veterans Affairs (CARA-029-09F), the American Heart Association (10034439) and the University of Utah Research Foundation supported FV and MAM.

Author Contributions

N.B. first described this syndrome in 1973. F. C. L. and his laboratory have pursued this project since 1994. O.T., H.R.T., H.S., J.J., J.T., H.H., R.H., L.H. and R.N. phenotyped the syndrome. D.C., M.G.B., G.P., M.H. and H.R.T. identified additional families with the syndrome. T.F.W., J.O., S.B., A.B. and F.R. performed microsatellite and SNP linkage analyses. M.G. and N.H. performed genotyping analyses within the families and also analyzed Chinese hypertensive families that link to the chromosome 12p locus. A.W., M.K., A.R., K.R. and T.L. performed cytogenetics. S.S. performed *in situ* mouse studies. S.M., P.M.K., D.P. and J.H. did Illumina whole-genome sequencing. A.A, P.G.M. and S.B. analyzed Complete Genomics whole-genome sequencing data and A.A. identified the *PDE3A* mutation. H.S. statistically analyzed various data. C.L. and A.A. performed the confocal immunofluorescence imaging. F.Q., I.H., E.B.-K., and A.M. performed technical studies. K.M. and Y.W.-N. prepared MSC. M.V. kindly provided non-affected MSC and supported all the MSC investigations. Y.W.-N., A.A. and P.G.M. analyzed cell proliferation. F.V. and M.A.M. kindly provided FLAG-tagged PDE3A expression constructs and have provided intellectual input. C.S. and E.K. performed ELISA assays on recombinant proteins and peptide spot assays. P.G.M. participated in all scientific aspects of the study and personally was responsible for the PDE3A functional assays, IC_{50} determinations, and work with MSCs. P.G.M., F.C.L. and S.B. wrote the manuscript. The manuscript was the product of >20 years' research to which all authors have contributed.

Disclosure statement

The authors have nothing to disclose.

References

1. Hunter, D.J. & Reddy, K.S. Noncommunicable Diseases. *N Engl J Med* **369**, 1336-1343 (2013).
2. Schuster, H. *et al.* Severe autosomal dominant hypertension and brachydactyly in a unique Turkish kindred maps to human chromosome 12. *Nat Genet* **13**, 98-100 (1996).
3. Schuster, H. *et al.* A cross-over medication trial for patients with autosomal-dominant hypertension with brachydactyly. *Kidney Int* **53**, 167-72 (1998).
4. Naraghi, R. *et al.* Neurovascular compression at the ventrolateral medulla in autosomal dominant hypertension and brachydactyly. *Stroke* **28**, 1749-54 (1997).
5. Lifton, R.P. Genetic dissection of human blood pressure variation: common pathways from rare phenotypes. *Harvey Lect* **100**, 71-101 (2004).
6. Bilginturan, N., Zileli, S., Karacadag, S. & Pirnar, T. Hereditary brachydactyly associated with hypertension. *J Med Genet* **10**, 253-9 (1973).
7. Toka, O. *et al.* Childhood hypertension in autosomal-dominant hypertension with brachydactyly. *Hypertension* **56**, 988-94 (2010).
8. Bahring, S. *et al.* Autosomal-dominant hypertension with type E brachydactyly is caused by rearrangement on the short arm of chromosome 12. *Hypertension* **43**, 471-6 (2004).
9. Bahring, S. *et al.* Inversion region for hypertension and brachydactyly on chromosome 12p features multiple splicing and noncoding RNA. *Hypertension* **51**, 426-31 (2008).
10. Gong, M. *et al.* Genome-wide linkage reveals a locus for human essential (primary) hypertension on chromosome 12p. *Hum Mol Genet* **12**, 1273-7 (2003).
11. Maurice, D.H. *et al.* Cyclic nucleotide phosphodiesterase activity, expression, and targeting in cells of the cardiovascular system. *Mol Pharmacol* **64**, 533-46 (2003).
12. Wakabayashi, S. *et al.* Involvement of phosphodiesterase isozymes in osteoblastic differentiation. *J Bone Miner Res* **17**, 249-56 (2002).
13. Michot, C. *et al.* Exome sequencing identifies PDE4D mutations as another cause of acrodysostosis. *Am J Hum Genet* **90**, 740-5 (2012).
14. Lee, H. *et al.* Exome sequencing identifies PDE4D mutations in acrodysostosis. *Am J Hum Genet* **90**, 746-51 (2012).

15. Maass, P.G. *et al.* A misplaced lncRNA causes brachydactyly in humans. *J Clin Invest* **122**, 3990-4002 (2012).
16. Insel, P.A., Stengel, D., Ferry, N. & Hanoune, J. Regulation of adenylate cyclase of human platelet membranes by forskolin. *J Biol Chem* **257**, 7485-90 (1982).
17. Knowles, R.G., Palacios, M., Palmer, R.M. & Moncada, S. Formation of nitric oxide from L-arginine in the central nervous system: a transduction mechanism for stimulation of the soluble guanylate cyclase. *Proc Natl Acad Sci U S A* **86**, 5159-62 (1989).
18. Wechsler, J. *et al.* Isoforms of cyclic nucleotide phosphodiesterase PDE3A in cardiac myocytes. *J Biol Chem* **277**, 38072-8 (2002).
19. Vandeput, F. *et al.* Selective regulation of cyclic nucleotide phosphodiesterase PDE3A isoforms. *Proc Natl Acad Sci U S A* **110**, 19778-83 (2013).
20. Choi, Y.H. *et al.* Identification of a novel isoform of the cyclic-nucleotide phosphodiesterase PDE3A expressed in vascular smooth-muscle myocytes. *Biochem J* **353**, 41-50 (2001).
21. Cone, J. *et al.* Comparison of the effects of cilostazol and milrinone on intracellular cAMP levels and cellular function in platelets and cardiac cells. *J Cardiovasc Pharmacol* **34**, 497-504 (1999).
22. Dunkerley, H.A. *et al.* Reduced phosphodiesterase 3 activity and phosphodiesterase 3A level in synthetic vascular smooth muscle cells: implications for use of phosphodiesterase 3 inhibitors in cardiovascular tissues. *Mol Pharmacol* **61**, 1033-40 (2002).
23. Linglart, A. *et al.* Recurrent PRKAR1A mutation in acrodysostosis with hormone resistance. *N Engl J Med* **364**, 2218-26 (2011).
24. Salem, H.K. & Thiemermann, C. Mesenchymal stromal cells: current understanding and clinical status. *Stem Cells* **28**, 585-96 (2010).
25. Begum, N., Hockman, S. & Manganiello, V.C. Phosphodiesterase 3A (PDE3A) deletion suppresses proliferation of cultured murine vascular smooth muscle cells (VSMCs) via inhibition of mitogen-activated protein kinase (MAPK) signaling and alterations in critical cell cycle regulatory proteins. *J Biol Chem* **286**, 26238-49 (2011).
26. Schuster, H. *et al.* Autosomal dominant hypertension and brachydactyly in a Turkish kindred resembles essential hypertension. *Hypertension* **28**, 1085-92 (1996).

27. Hunter, R.W., Mackintosh, C. & Hers, I. Protein kinase C-mediated phosphorylation and activation of PDE3A regulate cAMP levels in human platelets. *J Biol Chem* **284**, 12339-48 (2009).
28. Pozuelo Rubio, M., Campbell, D.G., Morrice, N.A. & Mackintosh, C. Phosphodiesterase 3A binds to 14-3-3 proteins in response to PMA-induced phosphorylation of Ser428. *Biochem J* **392**, 163-72 (2005).
29. Castagna, M. *et al.* Direct activation of calcium-activated, phospholipid-dependent protein kinase by tumor-promoting phorbol esters. *J Biol Chem* **257**, 7847-51 (1982).
30. Graves, L.M. *et al.* Protein kinase A antagonizes platelet-derived growth factor-induced signaling by mitogen-activated protein kinase in human arterial smooth muscle cells. *Proc Natl Acad Sci U S A* **90**, 10300-4 (1993).
31. Zhao, H., Guan, Q., Smith, C.J. & Quilley, J. Increased phosphodiesterase 3A/4B expression after angioplasty and the effect on VASP phosphorylation. *Eur J Pharmacol* **590**, 29-35 (2008).
32. Song, G.J., Fiaschi-Taesch, N. & Bisello, A. Endogenous parathyroid hormone-related protein regulates the expression of PTH type 1 receptor and proliferation of vascular smooth muscle cells. *Mol Endocrinol* **23**, 1681-90 (2009).
33. Hundsrucker, C. *et al.* Glycogen synthase kinase 3beta interaction protein functions as an A-kinase anchoring protein. *J Biol Chem* **285**, 5507-21 (2010).
34. Beca, S. *et al.* Phosphodiesterase type 3A regulates basal myocardial contractility through interacting with sarcoplasmic reticulum calcium ATPase type 2a signaling complexes in mouse heart. *Circ Res* **112**, 289-97 (2013).
35. Lygren, B. *et al.* AKAP complex regulates Ca2+ re-uptake into heart sarcoplasmic reticulum. *EMBO Rep* **8**, 1061-7 (2007).
36. Bassler, D., Kreutzer, K., McNamara, P. & Kirpalani, H. Milrinone for persistent pulmonary hypertension of the newborn. *Cochrane Database Syst Rev*, CD007802 (2010).
37. Pfitzer, G. Invited review: regulation of myosin phosphorylation in smooth muscle. *J Appl Physiol (1985)* **91**, 497-503 (2001).
38. Klopocki, E. *et al.* Deletion and point mutations of PTHLH cause brachydactyly type E. *Am J Hum Genet* **86**, 434-9 (2010).

39. Bastepe, M. *et al.* Stimulatory G protein directly regulates hypertrophic differentiation of growth plate cartilage in vivo. *Proc Natl Acad Sci U S A* **101**, 14794-9 (2004).
40. Chilco, P.J., Leopold, V. & Zajac, J.D. Differential regulation of the parathyroid hormone-related protein gene P1 and P3 promoters by cAMP. *Mol Cell Endocrinol* **138**, 173-84 (1998).
41. Smolenski, A., Poller, W., Walter, U. & Lohmann, S.M. Regulation of human endothelial cell focal adhesion sites and migration by cGMP-dependent protein kinase I. *J Biol Chem* **275**, 25723-32 (2000).

Figures

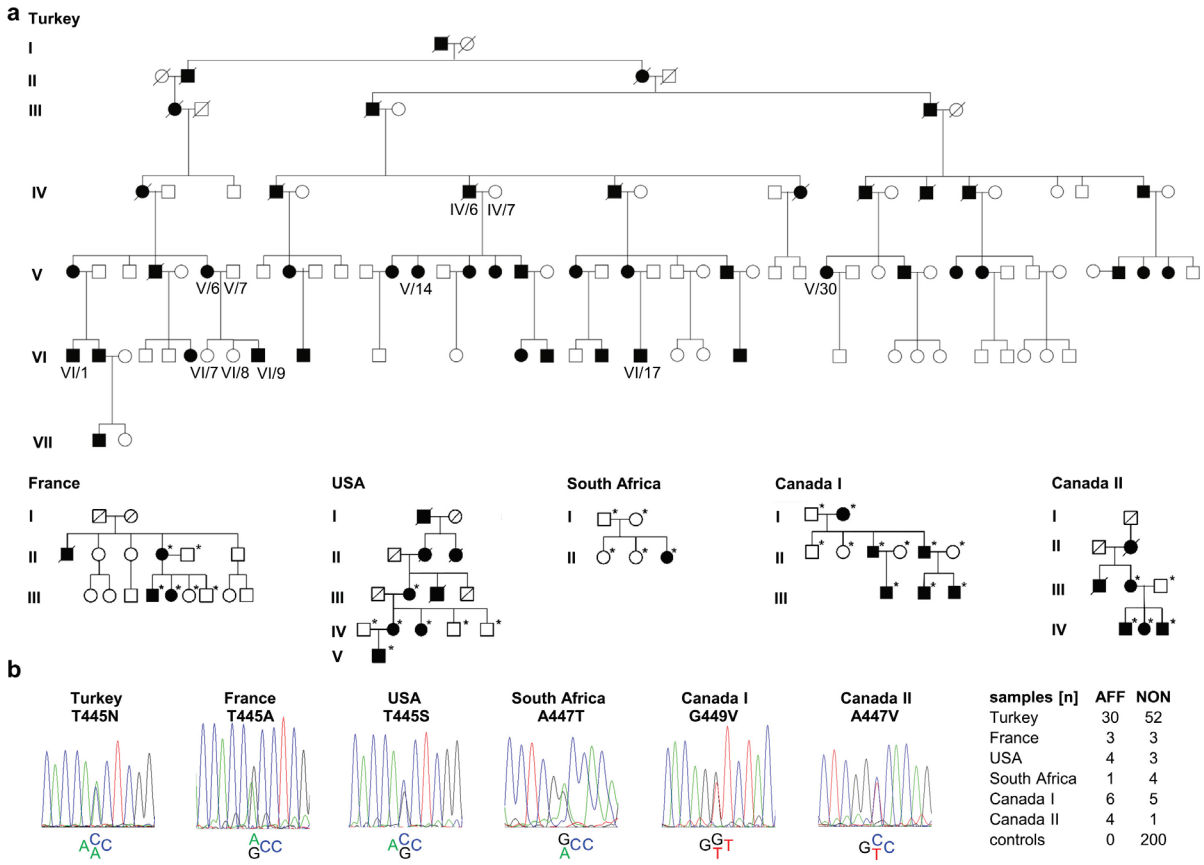

Figure 1. Pedigrees and *PDE3A* missense mutations in six unrelated families with autosomal-dominant hypertension with brachydactyly type E (HTNB).

(a) The genomes of the Turkish family members IV/6, IV/7, V/14 and V/30 were sequenced. DNA from all affected and non-affected Turkish family members was used for *PDE3A* Sanger sequencing. The asterisks in the pedigrees of the other families indicate *PDE3A* re-sequencing of family members. In all affected persons (black symbols) a *PDE3A* mutation was found in comparison to their non-affected related family members (white symbols), demonstrating complete penetrance in all families. The nuclear family of V/6+7 and VI/7-9 was used for haplotype analysis. X-rays of VI/1 and VI/9 are shown in Figure 2b. MSC were extracted from VI/9 and VI/17. **(b)** Six different *PDE3A* missense mutations introduced amino-acid

changes at positions 445, 447, and 449; total number of samples analyzed; AFF = affected persons, NON = non-affected controls

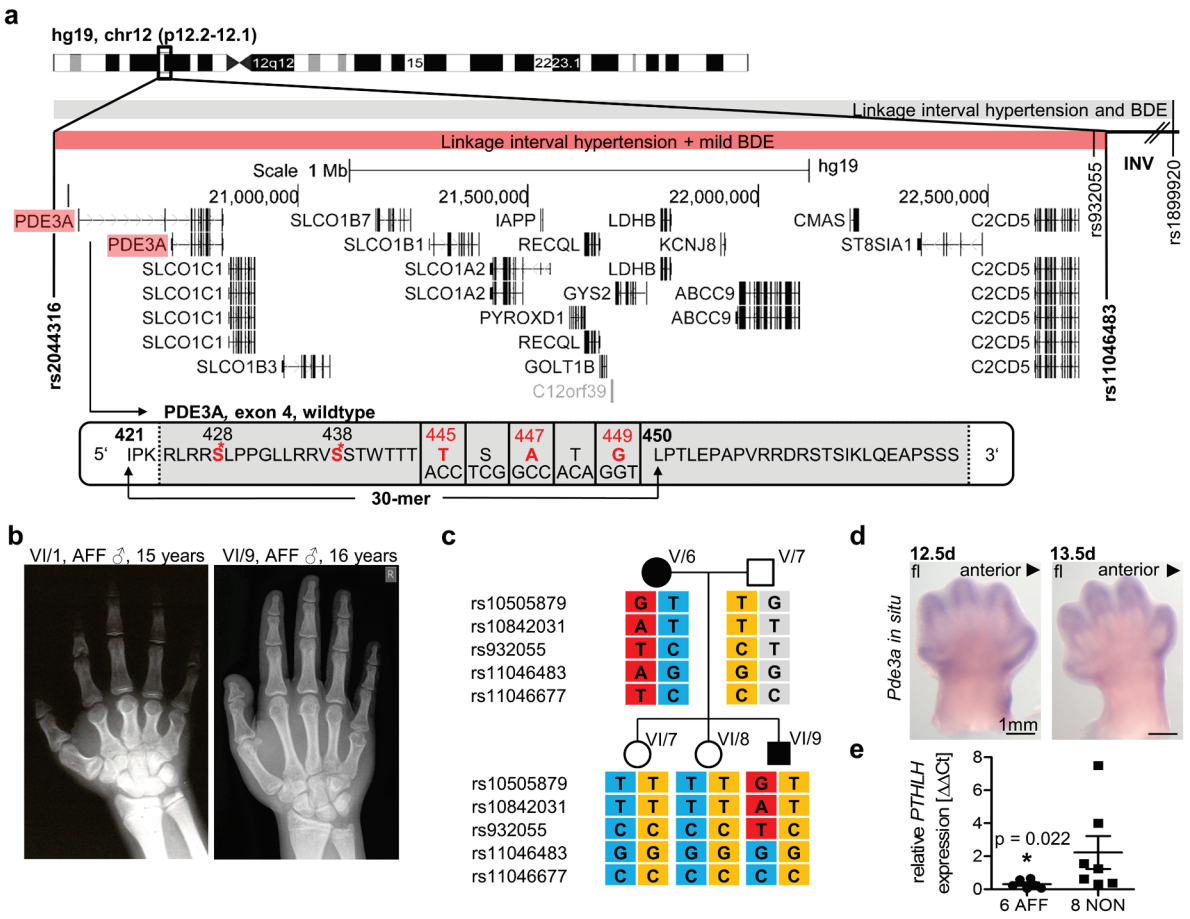

Figure 2. The linkage interval of HTNB and *Pde3a*, and *PTHLH* in chondrogenesis.

(a) The linkage interval of all families (grey bar) with flanking SNPs on chromosome 12p12.2-12.1 and the previously described inversion (INV) is shown (human genome assembly hg19). The red bar shows the linkage interval of a hypertensive boy with mild BDE and near-average height for age (VI/9, panel c) with all annotated RefSeq genes. The peptide sequence of PDE3A exon 4 harboring the mutations (amino acids 445, 447 and 449) and the phosphorylation sites Ser$^{428+438}$ near the mutations is shown. The sequence of PDE3A Iso^{421}-Leu^{450} (30-mer peptide) was used for peptide SPOT assays (Fig. 5 and Supplementary Fig. 13, 14). **(b)** Mild BDE of VI/9 and of his cousin VI/1 that was far more severe. **(c)** A haplotype analysis of the Turkish nuclear family identified a novel recombination excluding the inversion from linkage in VI/9 (black square), compared to his mother V/6 (black circle). **(d)**

The chondrogenic *Pde3a* expression in developing mice at 12.5d and 13.5d was studied by RNA *in situ* hybridizations. *Pde3a* was expressed in domains involved in digit formation. **(e)** The BDE-associated *PTHLH* was downregulated in chondrogenically-induced fibroblasts from 6 age and gender-matched affected persons *versus* 8 non-affected controls (mean±SEM, Wilcoxon-Mann-Whitney rank sum test, $p = 0.022$).

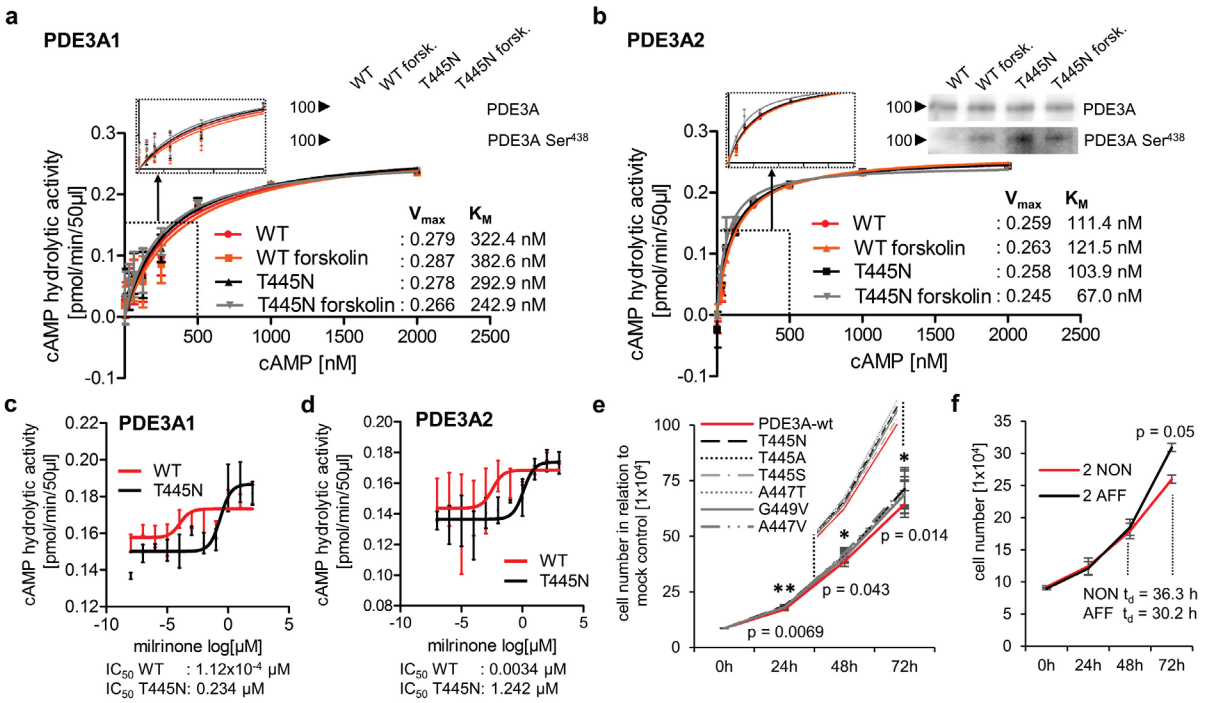

Figure 3. Michaelis-Menten kinetics and IC_{50} measurements, and CFSE proliferation assays. HeLa cells were transiently transfected to express FLAG-tagged wildtype (WT) or the T445N PDE3A mutation. Recombinant PDE3A1 or PDE3A2 proteins were purified via their FLAG-tags. **(a)** In Michaelis-Menten kinetics of PDE3A1 and **(b)** of PDE3A2, V_{max} and K_M revealed that the T445N mutation purified from non-stimulated and forskolin-stimulated cells displayed increased cAMP-affinity compared to PDE3A WT (n = 3). **(c)** For the inhibitor milrinone, the IC_{50} for PDE3A1 WT was $1.12x10^{-4}$ µM, in contrast to 0.234 µM for the T445N mutant (n = 3). **(d)** For PDE3A2 WT the IC_{50} for milrinone was 0.0034 µM, in comparison to 1.242 µM for PDE3A2 T445N (n = 2). **(e)** A proliferation assay elucidated increased mitosis for all the six *PDE3A* mutations compared to *PDE3A* wildtype after expression in HeLa cells (mean±SEM of n = 3, Wilcoxon-Mann-Whitney rank sum test, $p<0.01$, $p<0.05$). The difference in cell numbers between mutational PDE3A and wildtype cells was modest 6.2 % and maximum 9.5 %. **(f)** Proliferation assay of two patient-derived VSMC (AFF) and two controls (NON). The patients' VSMC proliferated faster than the

controls, doubling time (t_d) for NON was 36.3 h and 30.2 h for AFF (means±SEM of n = 3, Wilcoxon-Mann-Whitney test, p = 0.05). The functional assays in Figure 3 were biological replicates.

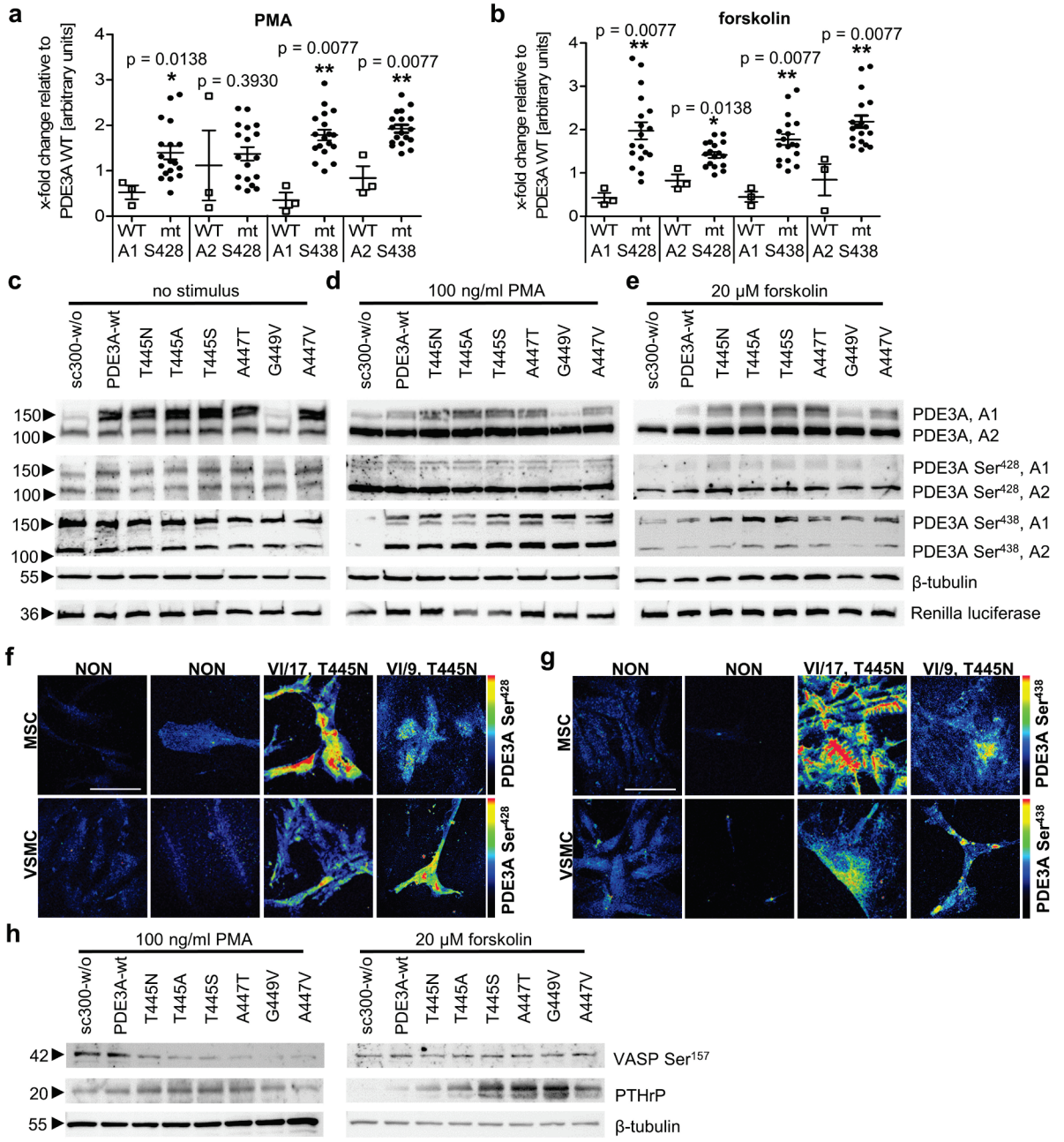

Figure 4. PDE3A Ser$^{428+438}$ phosphorylation in HeLa cells transfected with full-length *PDE3A*, in MSC and in MSC-derived VSMC.

(a) In densitometrical Western blotting quantifications of PMA-stimulated, and (**b**) forskolin-treated HeLa, significant differences between transfected wildtype (WT) and each mutational PDE3A at Ser^{428} and Ser^{438} were determined after normalization to β-tubulin. PDE3A mutational signal differences are shown as fold changes relative to the expression of

transfected PDE3A WT. The phosphorylation of mutational PDE3A1 and PDE3A2 (mt) were increased compared to wildtype (WT), (mean±SEM of n = 3, two-tailed Wilcoxon-Mann-Whitney test, ** $p<0.01$, * $p<0.05$). (**c**) HeLa cells transiently expressing the six PDE3A mutations were non-stimulated, (**d**) stimulated with PMA to induce PKC, or (**e**) treated with forskolin to activate PKA. Detection of expression of co-transfected Renilla luciferase confirmed equal transfection conditions; β-tubulin was loading control. Anti-PDE3A antibodies detected the isoforms A1 and A2. Experimental and variation differences in phosphorylation were detected upon quantification and normalization to the loading control and are summarized in the scatter plots of panel a and b; single values are given in Supplemental Fig. S10. **(f)** Differences in phosphorylated PDE3A residues Ser^{428} and **(g)** Ser^{438} were documented between two non-affected controls (NON) and two affected persons (AFF) using semi-quantitative immuno-fluorescence. The pseudo-color spectrum indicates signal intensities from low (black) to high (red). PDE3A was highly phosphorylated in the T445N AFF compared to NON, in MSC and VSMC. Scale bar = 50 μm. **(h)** PMA and forskolin stimulation of transfected HeLa. PMA stimulation caused reduced PKA-mediated VASP Ser^{157} phosphorylation and higher PTHrP expression in cells expressing the PDE3A mutants. The expression of non-phosphorylated VASP did not change. Western blots for quantifications were biological replicates from three independent experiments.

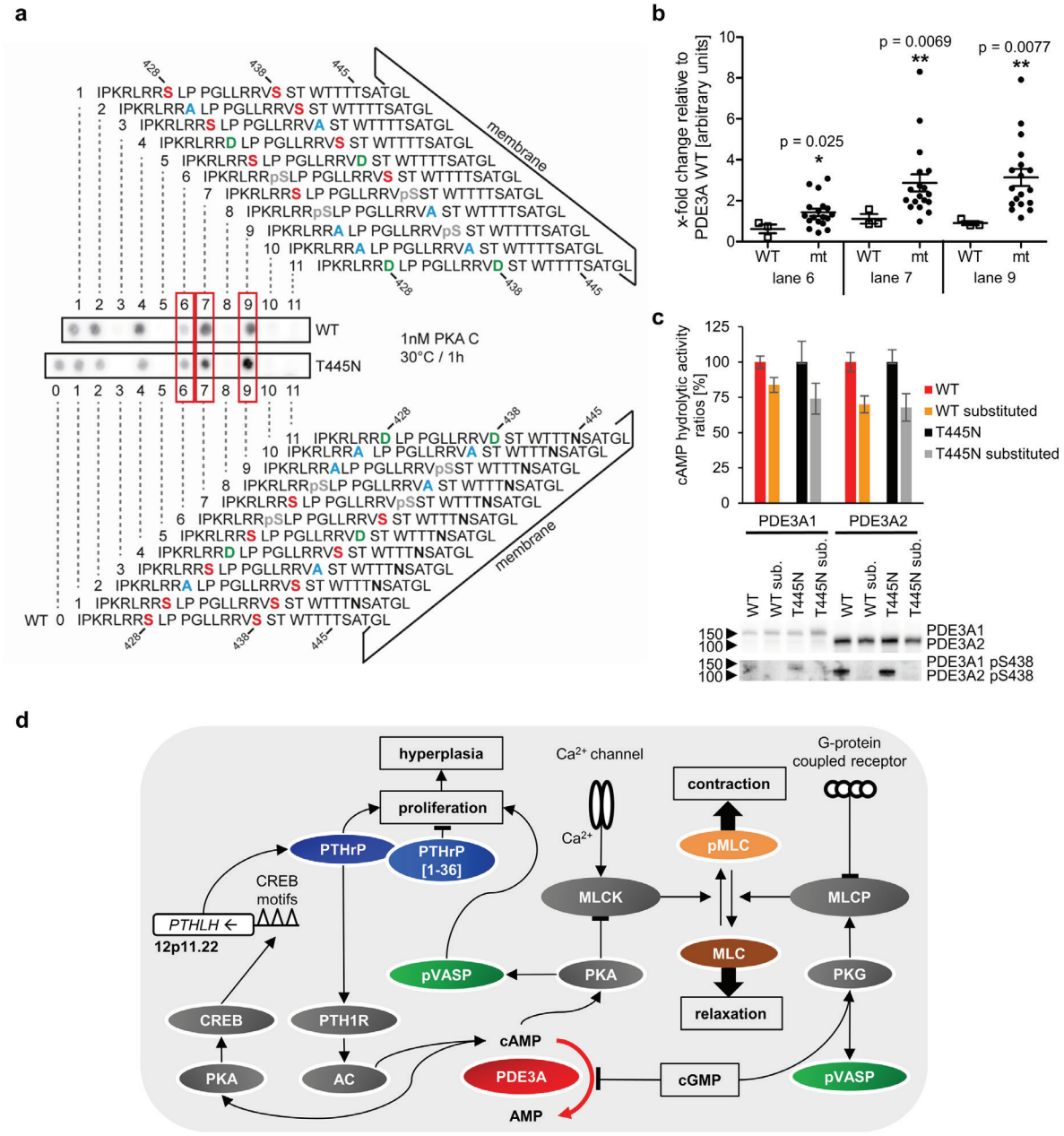

Figure 5. Peptide SPOT assay of the *PDE3A* mutation T445N.

(a) PDE3A wildtype (WT) and PDE3A T445N mutant peptides representing Iso^{421}-Leu^{450} were spot-synthesized (sequences in Supplementary Fig. 13a). Ser$^{428+438}$ were replaced by alanine (A) and asparagine (D) as indicated. For visual simplicity, signals of PDE3A wildtype *versus* PDE3A T445N mutation are shown; remaining mutations' peptide spots are shown in Supplementary Fig. 13b. PKA phosphorylation of pre-phosphorylated (pS) Ser^{428} showed

higher serine (S) Ser^{438} phosphorylation of the T445N mutant (lane 6). Pre-phosphorylated Ser^{438} and subsequent PKA incubation also caused enhanced phosphorylation signals of all PDE3A mutations (lane 7 and 9; Supplementary Fig. 13b). **(b)** Densitometrical quantification of peptide spots of all mutants. The signals of lanes 6, 7 and 9 showed significantly enhanced phosphorylation after PKA incubation (mean±SEM of biological replicates n = 3, two-tailed Wilcoxon-Mann-Whitney rank sum test, ** $p<0.01$, * $p<0.05$). **(c)** Michaelis-Menten (MM) kinetics of FLAG-tagged PDE3A1 and PDE3A2 wildtype (WT) and T445N in comparison to FLAG-tagged PDE3A isoforms substituted (sub.) with alanines at position 428, 438, 439 and 440. The substitutions led to a decrease in the cAMP affinity and cAMP hydrolysis (mean±SD of biological replicates n = 3). The data shown are the ratios of phosphorylated PDE3A wildtype (WT) or T445N versus their substituted isoforms in percent. Western blotting validated equal PDE3A amounts during functional MM-kinetics and diminished Ser^{438}phosphorylation upon alanine substitutions. **(d)** Compendious scheme for the PDE3A involvement in VSMC and chondrocytes. In VSMC, the myosin light-chain kinase (MLCK) and the myosin light chain phosphatase (MLCP) act in concert to phosphorylate and dephosphorylate the myosin light chain (MLC) for vascular contraction and relaxation, respectively.[37] PKA and protein kinase G (PKG) activate VASP by phosphorylation of Ser^{157} and Ser^{239}, respectively.[41] Reduced VASP Ser^{157} phosphorylation and higher PDE3A activity were associated with enhanced VSMC proliferation that accounts for vessel wall hyperplasia.[31] Full-length PTHrP stimulated whilst PTHrP [1-36] repressed the VSMC proliferation.[32] CREB binding to the *PTHLH* promoter regulates *PTHLH* expression in a cAMP-dependent manner. The encoded protein PTHrP transduces signals through the PTH1R (PTH/PTHrP) receptor in chondrocytes and activates Gs-α, thereby stimulating the adenylate

cyclase (AC) to produce cAMP.[39] Since PDE3A hydrolyses cAMP, PKA is cAMP-dependently regulated and activates CREB, which in turn regulates the *PTHLH* expression.[40]